

# Short-Term Differentiation of Glioblastoma Stem Cells Induces Hypoxia Tolerance

Håvard K. Skjellegrind<sup>1</sup> · Artem Fayzullin<sup>1</sup> · Erik O. Johnsen<sup>2</sup> · Lars Eide<sup>3</sup> · Iver A. Langmoen<sup>1</sup> · Morten C. Moe<sup>2</sup> · Einar O. Vik-Mo<sup>1</sup>

Received: 26 October 2015 / Revised: 3 February 2016 / Accepted: 8 February 2016 / Published online: 25 February 2016  
© The Author(s) 2016. This article is published with open access at Springerlink.com

**Abstract** Glioblastoma is the most common and malignant brain cancer. In spite of surgical removal, radiation and chemotherapy, this cancer recurs within short time and median survival after diagnosis is less than a year. Glioblastoma stem cells (GSCs) left in the brain after surgery is thought to explain the inevitable recurrence of the tumor. Although hypoxia is a prime factor contributing to treatment resistance in many cancers, its effect on GSC has been little studied. Especially how differentiation influences the tolerance to acute hypoxia in GSCs is not well explored. We cultured GSCs from three patient biopsies and exposed these and their differentiated (1- and 4-weeks) progeny to acute hypoxia while monitoring intracellular calcium and mitochondrial membrane potential ( $\Delta\Psi_m$ ). Undifferentiated GSCs were not hypoxia tolerant, showing both calcium overload and mitochondrial depolarization. One week differentiated cells were the most tolerant to hypoxia, preserving intracellular calcium stability and  $\Delta\Psi_m$  during 15 min of acute hypoxia. After 4 weeks of differentiation, mitochondrial mass was

significantly reduced. In these cells calcium homeostasis was maintained during hypoxia, although the mitochondria were depolarized, suggesting a reduced mitochondrial dependency. Basal metabolic rate increased by differentiation, however, low oxygen consumption and high  $\Delta\Psi_m$  in undifferentiated GSCs did not provide hypoxia tolerance. The results suggest that undifferentiated GSCs are oxygen dependent, and that limited differentiation induces relative hypoxia tolerance. Hypoxia tolerance may be a factor involved in high-grade malignancy. This warrants a careful approach to differentiation as a glioblastoma treatment strategy.

**Keywords** Brain cancer stem cell · Hypoxia tolerance · Differentiation · Glioblastoma · GSC · Anoxia

## Introduction

Glioblastoma multiforme (GBM) is the most common primary brain cancer. Current treatment combines surgery, radiation and chemotherapy. Median survival is less than 10 months in unselected patient groups [1]. The isolation of glioma cells possessing stem cell properties has shed new light on this cancer [2, 3]. Glioblastoma stem cells (GSCs) have shown resistant to both radio- and chemotherapy [4–6]. GSCs left in the brain after tumor surgery is currently the leading theory explaining inevitable tumor recurrence [6]. Targeting the cells migrating from the tumor and surviving radiation and chemotherapy seems required for success. However, the true identity of these cells is not known. Chemo- and radio-resistance in gliomas is promoted by hypoxia [7] and the cells most resistant to treatment are found in the hypoxic parts of glioblastoma tumors [8]. Severe tumor hypoxia is associated with poor

**Electronic supplementary material** The online version of this article (doi:10.1007/s11064-016-1868-2) contains supplementary material, which is available to authorized users.

✉ Håvard K. Skjellegrind  
havard.skjellegrind@ntnu.no

- <sup>1</sup> Vilhelm Magnus Laboratory for Neurosurgical Research, Department of Neurosurgery and Institute for Surgical Research, Oslo University Hospital, Oslo, Norway
- <sup>2</sup> Center for Eye Research, Department of Ophthalmology, Oslo University Hospital, Oslo, Norway
- <sup>3</sup> Department of Medical Biochemistry, University of Oslo, Oslo, Norway

survival in both glioblastoma [9, 10] and several other cancers [11, 12]. It is therefore crucial to identify the cells that are most capable to survive in hypoxic conditions.

The effects of acute and chronic hypoxia on malignant cells can be different. Studies using cell culture in moderate chronic hypoxia (1–2 % O<sub>2</sub>) have shown enrichment of stem like cells in both glioma [13, 14] and other cancers [15, 16]. Acute, severe hypoxia (0–0.5 % O<sub>2</sub>) induces more cell death and thus strict selection of tolerant clones. Malignant progression has been found in many studies of acute tumor hypoxia, reviewed in [17]. Specifically, the histological features of glioblastoma including thrombosed vessels and pseudopallisading necrosis suggest that acute severe hypoxia has a central role in tumorigenesis [18]. Metabolic responses to acute hypoxia differ from that of chronic hypoxia [19]. Tolerance to acute hypoxia, however, is still a little explored phenomenon in cancer stem cells.

Differentiation is suggested as a potential treatment modality addressing GSCs [20]. However, in studies where immature cells have been transplanted to animals, both we and others have found better survival and integration of partially differentiated cells compared to undifferentiated cells [21–23]. The setting of transplantation itself is a hypoxic situation to the grafted cells, and tolerance to low oxygen supply could be important for survival and integration. Also in cancer metastasis, migrating cells would encounter low oxygen areas, and hypoxia tolerance could be important for the invasiveness of the cells. However, knowledge about hypoxia tolerance is limited. We have previously found increased resistance to hypoxia in immature brain cells [24]. The objective for this study was to investigate whether GCSs tolerate acute hypoxia and how differentiation influences their hypoxia tolerance.

## Methods and Materials

### Cell Culture

Glioblastoma biopsies were obtained from three informed and consenting patients during tumor surgery. Tissue harvesting was approved by the Norwegian Regional Committee for Medical Research Ethics (07321b). The biopsies were treated as previously described [25]. Briefly, the biopsies underwent mechanical and enzymatic dissociation before culture at 37 °C, 5 % CO<sub>2</sub> in DMEM/F12 (Invitrogen) supplemented with 2 % B27 without retinoic acid (Invitrogen), 1 % HEPES (Lonza), 0.5 % heparin (Leo pharma), 100 U/ml streptomycin (Lonza), 100 U/ml penicillin (Lonza), 10 ng/ml bFGF (R&D Systems) and 20 ng/ml EGF (R&D Systems). For each passage, the cells were dissociated using trypsin (Invitrogen) before plating at

$5.0 \times 10^4$  cells/ml in 10 ml medium in 75 cm<sup>2</sup> low adhesion flasks (Nunc). For induction of differentiation the medium contained DMEM/F12 with HEPES, Heparin, streptomycin, and penicillin as above, in addition to 4 % serum and 2 % B27 with retinoic acid, as previously described [26]. Glass slides and dishes were coated with Fibronectin 10 µg/ml (Sigma) in PBS. GSCs were differentiated for 1 or 4 weeks.

### Immunocytochemistry

GSCs were plated at 1600 cells/cm<sup>2</sup> in fibronectin coated glass bottom dishes (WillCo-dish 40 mm, WillCo Wells). Undifferentiated cells were allowed 2 days to settle on the coated surface. Differentiated cells were fixed after 1 and 4 weeks. Cells were washed in PBS and fixed in 4 % paraformaldehyde. Permeabilization in 0.1 % Triton-X for 5 min before blocking with 5 % bovine serum albumin (BSA), 5 % donkey serum and 0.1 % Triton-X for 30 min. The primary antibodies reactive against  $\beta$ III-tubulin (rabbit 1:1000, Sigma), nestin (goat 1:500), MAP-2 (mouse 1:500, Chemicon), GFAP (rabbit 1:1000, Dako), Ki-67 (mouse 1:1000) were diluted in PBS with 0.5 % BSA, 0.5 % donkey serum and 0.1 % Tween 20 and incubated overnight at 4 °C. Secondary antibodies, anti-mouse Alexa 488 (donkey 1:500, Invitrogen) anti-rabbit Alexa 555 (donkey 1:500, Invitrogen) and anti-goat Alexa 647 (donkey 1:500, Invitrogen), were incubated for 1 h at 20 °C. Nuclear staining was done using Hoechst 33258 (1:5000, Sigma).

### Fluorescence Imaging

Immunostained cells were imaged using an Olympus IX81 inverted fluorescence microscope equipped with excitation and emission filters for blue (ex: 350/50, em: 460/20), green (ex: 470/40, em: 515/30), red (ex: 545/30, em: 610/75) and deep red (ex: 620/60, em: 700/75). Images were acquired using Olympus soft imaging xcellence software. Post processing of the fluorescence images was done using the ImageJ package Fiji. All images presented for comparison were stained, imaged and processed identically.

### Time-Lapse Fluorescence Imaging

Cells were plated at a density of 500 cells/cm<sup>2</sup> on fibronectin coated glass slides. To enable rapid exchange of medium, the slides were attached to a flow chamber. Perfusion fluid was artificial cerebrospinal fluid (ACSF) with the following composition (in mM): NaCl: 123; KCl: 3.75; KH<sub>2</sub>PO<sub>4</sub>: 1.25; NaHCO<sub>3</sub>: 26; dextrose: 10; MgCl<sub>2</sub>: 1 and CaCl<sub>2</sub>: 2 [27]. pH was controlled by CO<sub>2</sub> perfusion. Before imaging the cells were incubated with 30 µM Rhodamine

123 (Rh123) to monitor mitochondrial membrane potential ( $\Delta\Psi_m$ ) [28] and 2  $\mu\text{M}$  Fura-2/AM for  $\text{Ca}^{2+}$  imaging [29]. Time-lapse imaging was done using an Olympus IX81 inverted fluorescence microscope with temperature control. Rh123 was imaged using 492/18 nm excitation and 531/32 nm emission filters. Phototoxicity and photobleaching were reduced by using a 3.9 % neutral density (ND) filter. Fura-2 was excited at 340/15 and 380/15 nm (11 % ND) and recorded using a 510/40 emission filter. For hypoxia solutions, oxygen was removed by  $\text{N}_2$  perfusion before addition of an oxygen scavenger, sodium dithionite (0.75 mM; Sigma-Aldrich). Scavenger toxicity was ruled out by control experiments using oxygenated ACSF containing sodium dithionite. After hypoxia 1  $\mu\text{M}$  Carbonyl cyanide 4-(trifluoromethoxy) phenylhydrazone (FCCP; Sigma) was used to totally depolarize the mitochondria [30], and thereby demonstrate any preserved  $\Delta\Psi_m$  by increase in Rh123 fluorescence. 5  $\mu\text{M}$  Ionomycin (Sigma) was used as a positive control of the  $[\text{Ca}^{2+}]_i$  recording. The cells were scored as lost or preserved  $\Delta\Psi_m$  and stable or unstable  $[\text{Ca}^{2+}]_i$ . Increase of the slope of Rh123 fluorescence after FCCP was used as the criterion for scoring preserved  $\Delta\Psi_m$ . Non-reversed increase of Fura-2 ratio within the hypoxia period was used as criteria for unstable  $[\text{Ca}^{2+}]_i$ .

### Computerized Analysis of Fluorescence Images

Ki-67 labeled cells were quantified using the open source image analysis software CellProfiler [31]. Hoechst and Ki-67 images were thresholded. Nuclei (Hoechst) and Ki-67 positive nuclei were identified as primary objects. Hoechst and Ki-67 labeling were related as parent and child objects. Ki-67 positive and negative cells were thereby counted using the same criteria in both undifferentiated, 1 week differentiated and 4 weeks differentiated cultures.  $\geq 4$  experiments and more than 600 cells were counted in each experimental group.

### Gene Expression Analyses

Undifferentiated and differentiated cells were washed in PBS twice. The cells were further lysed by QiAzol (Qiagen) and stored at  $-20^\circ\text{C}$ . Total RNA was extracted using TRIzol Reagent according to the manufacturer's instructions (Life Technologies). RNA concentration and purity were measured using Nanodrop (Wilmington, DE). Reverse transcription was performed using the High Capacity cDNA Reverse Transcription Kit (Life Technologies), with 300 ng total RNA per 20  $\mu\text{l}$  reaction volume. qRT-PCR was performed using the StepOnePlus RT-PCR system (Life Technologies) and TaqMan Gene Expression Assays following protocols from the manufacturer (Life

Technologies). The thermo cycling conditions were  $95^\circ\text{C}$  for 10 min followed by 40 cycles of  $95^\circ\text{C}$  for 15 s. and  $60^\circ\text{C}$  for 1 min. The data were analyzed using the  $2^{-\Delta\Delta\text{Ct}}$  method as fold change relative to control, using GAPDH as endogenous control. All samples were run in duplicates. TaqMan Gene Expression assays include GFAP (Hs00909233\_m1), NES (Hs00707120\_s1), GAPDH (Hs99999905\_m1),  $\beta$ -III-tubulin (Hs00801390\_s1), and CD133 (Hs01009250-m1). Results are presented as fold change. Error bars are R-min/-max.

### Oxygen Consumption and Acidification Rate

Cells in all three groups of differentiation state were plated on SeaHorse 24 well plates at a density of  $5.0 \times 10^4$  cells/well 1 day before experiments. Medium was changed to buffer-free DMEM containing 2 mM glutamine, 5 mM pyruvate and 10 mM glucose 1 h before the start of the flux analyses. Simultaneous analyses of oxygen consumption rate (OCR) and extracellular acidification rate (ECAR) were performed on a Seahorse XF24-3 extracellular flux analyzer (Seahorse Bioscience). After baseline measurements, the following compounds were added with subsequent measurements: oligomycin (2  $\mu\text{g}/\text{ml}$ ), 2 additions of FCCP (1  $\mu\text{M}$ ), FCCP, rotenone (0.1  $\mu\text{M}$ ). Oxidative/glycolytic ratio was calculated by dividing average oxygen consumption rate (OCR) by extracellular acidification rate (ECAR). To ensure a valid comparison of OCR and ECAR, the cell numbers were confirmed by nuclear staining (as described under immunolabeling) after the flux measurements. Automated counting of cells after fluorescence microscopy was done as described above.

### Flow Cytometry

Flow cytometry was performed using an Accuri C6 flow cytometer. Live single cells were gated using forward and side scatter. From this population of cells mean fluorescence values were used.  $\Delta\Psi_m$  was measured using the ratiometric mitochondrial dye JC-1 [32]. Mitochondrial mass was quantified in methanol fixed cells using the fluorescent dye Nonyl Acridine Orange, that binds to cardiolipin in the inner mitochondrial membrane independently on energetic state [33] and with a linear relationship between dye incorporation and cardiolipin content [34]. Analysis of cytometry data was performed using FloJo software.

### Statistics

Rh123 fluorescence data were normalized and Fura-2 ratios calculated using MS Excel. Mean values from each experiment were used for statistics. The data were

transferred to GraphPad Prism 6.0 for statistics and presentation. ANOVA was used for statistical analysis of difference between groups. The hypoxia experimental groups consisted of at least five experiments each. Other experiments were conducted in triplicates or more. Results were considered significant where  $p < 0.05$ .

## Results

Experiments were performed using three different glioblastoma stem cell cultures obtained from three patients at primary surgical treatment without any previous oncological treatment. The three GSC cultures are referred to as T1, T2 and T3. Cells demonstrated self-renewal by exponential growth for 20 passages. The maintenance of tumorigenicity and expression of stem cell markers was maintained upon culturing under sphere-forming conditions [3, 25, 35].

Differentiation was assessed morphologically by immunolabeling and quantitatively by qPCR (Fig. 1). Immunocytochemistry displayed decreasing levels of the immature stem cell marker nestin, and to development of both neural and glial phenotype, shown by the neuronal marker  $\beta$ III-tubulin and glial marker GFAP. After 4 weeks differentiation a few cells also expressed the mature neuronal marker MAP-2. Ki-67, a marker of cellular proliferation was found in 45.0 % (38.5–51.6) of undifferentiated cells, 18.9 % (12.9–24.8) in 1 week and 11.6 % (6.2–17.1) in 4 weeks differentiated cells. In qPCR nestin expression was found significantly reduced after 4 weeks differentiation ( $p < 0.05$ ). The GSC marker CD133 expression was reduced at 1 week and further reduced at 4 weeks differentiation (both  $p < 0.01$ ).  $\beta$ III-tubulin expression increased significantly from undifferentiated state to 1 week differentiated ( $p < 0.01$ ). GFAP expression at 1-week differentiation was increased 28-fold compared to undifferentiated and still high at 4 weeks differentiation (21-fold).

Calcium deregulation is a widely used early indicator of neuronal death induced by ischemic stress [36]. In animals, reduced calcium response to hypoxia is regarded as a component of hypoxia tolerance [37]. As an indicator of hypoxia tolerance, we used the ability to maintain intracellular calcium integrity during hypoxia. This was measured by monitoring changes in fluorescence from the calcium indicator Fura-2. Figure 2a shows a representative trace of an undifferentiated GSC with Fura-2 ratio images from the different phases of the experiment. Figure 2b–d show traces of the Fura-2 ratio for each of the cells of the T1 tumor in experiments of undifferentiated (b), 1 week differentiated (c) and 4 weeks differentiated cells (d). The tumors T2 and T3 are shown in Online Resource 1. The

proportions of cells maintaining stable  $[Ca^{2+}]_i$  are shown for all three tumor cultures in Fig. 2e–g. Based on reports of hypoxia tolerance in immature neural cells [24, 38] and GSC enrichment in hypoxic tumor areas [8] we hypothesized that the most immature cells would tolerate hypoxia the best. The majority of undifferentiated GSCs, however, suffered from a sustained increase in  $[Ca^{2+}]_i$ . The proportions of cells maintaining stable  $[Ca^{2+}]_i$  in the three undifferentiated cultures were T1: 25.0 % (–11.4 to 61.3), T2: 47.7 % (14.8–80.5) and T3: 48.9 % (9.9–88.0; Fig. 2e–g). Thus, only a minority of the undifferentiated GSCs was able to maintain stable intracellular calcium during acute hypoxia.

A far lower proportion of differentiated GSCs revealed a  $[Ca^{2+}]_i$  increase that did not return to baseline level during hypoxia. 78.8 % (60.0–97.5) of T1 cells maintained stable calcium. For T2 and T3 the proportions were 96.7 % (87.4–105.9) and 100 % (100–100) respectively (Fig. 2e, f). Stability of  $[Ca^{2+}]_i$  was significantly better in the 1 week differentiated cells compared to the undifferentiated cells in all tumors tested (T1  $p < 0.001$ , T2 and T3  $p < 0.01$ , ANOVA).

From all three cultures of 4 weeks differentiated GSCs, all cells maintained intracellular calcium during the 15 min hypoxia period. Some of the cells had a small but transient increase, and then went back to baseline level. Ionomycin induced a twofold to threefold increase in Fura-2 ratio in all cells, demonstrating valid  $[Ca^{2+}]_i$  measurements. The difference compared to undifferentiated GSCs was significant for all three tumors (T1  $p < 0.001$ , T2 and T3  $p < 0.01$ , ANOVA).

Another early sign of fatal damage to brain cells is loss of mitochondrial membrane potential ( $\Delta\Psi_m$ ). Mitochondrial depolarization is an early step in programmed cell death and also a downstream event of temozolomide treatment [8], which is standard chemotherapy for glioblastoma patients. Mitochondrial function is thus a relevant indicator of hypoxia tolerance. The Warburg theory postulates independence of oxidative ATP production in cancer tissue. The dependence on mitochondrial energy metabolism in GSCs is not well studied. Before experimental hypoxia, the cells were incubated with both Fura-2 and the  $\Delta\Psi_m$  sensitive dye Rhodamine 123 (Rh123) and thus changes in  $\Delta\Psi_m$  could also be monitored. Figure 3a shows a representative recording of  $\Delta\Psi_m$  during hypoxia in an undifferentiated GSC. Figure 3b–d show the traces of Rh123 fluorescence from the single cells in the experiments on GSC culture T1. T2 and T3 are shown in Online Resource 2. The proportions of cells that preserved  $\Delta\Psi_m$  during hypoxia are shown in Fig. 3e–g. A large proportion of the undifferentiated cells exhibited early loss of mitochondrial membrane potential during hypoxia. This was shown by increase in cytoplasmic Rh123 fluorescence due



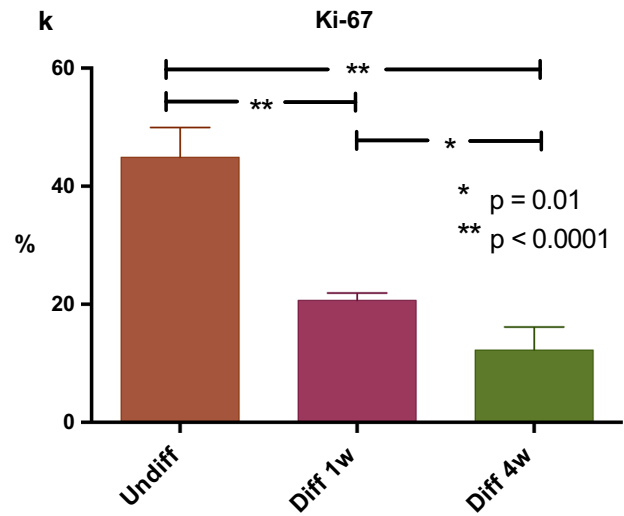
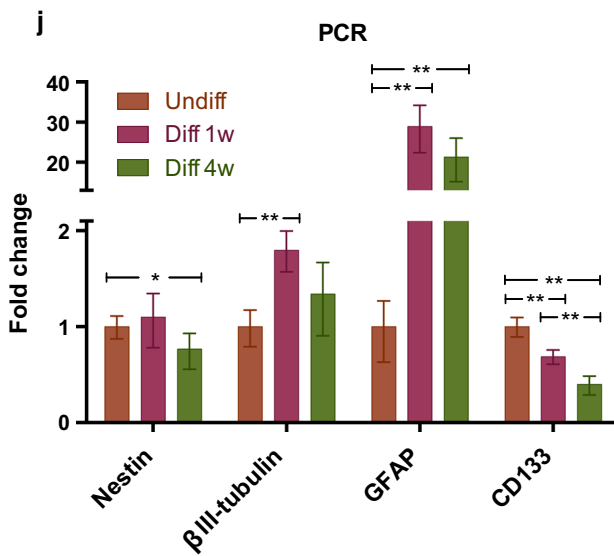
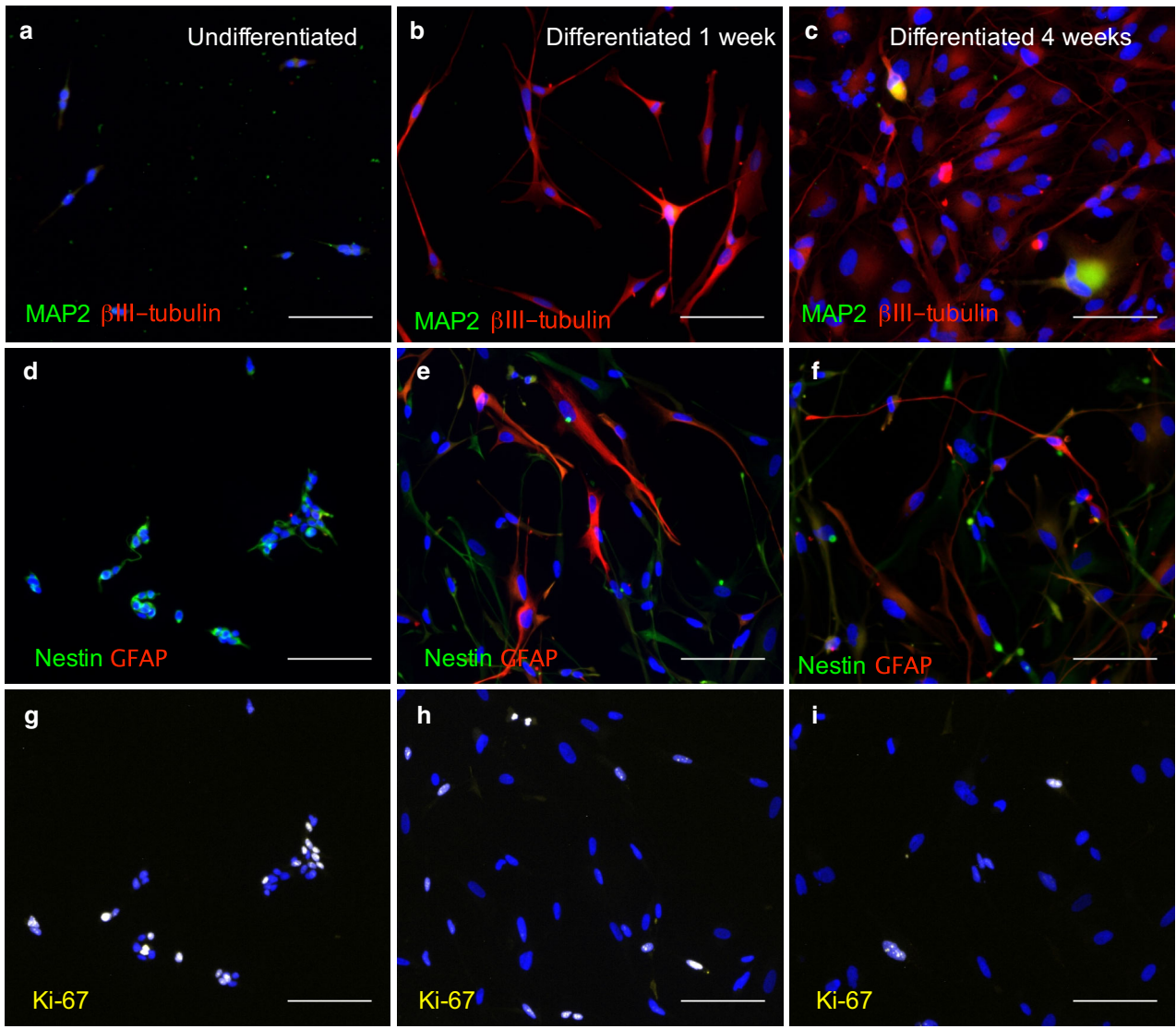


**Fig. 1** GSCs differentiation induced a more mature phenotype and reduced proliferation. Undifferentiated GSCs had highly positive staining of the neuronal stem cell marker nestin. Differentiation led to development of both neural and glial phenotype, shown by the neuronal marker  $\beta$ III-tubulin and glial marker GFAP. After 4 weeks differentiation a few cells also expressed the mature neuronal marker MAP-2. Proportions of immuno-reactive cells assessed by manual counting: **a** undifferentiated GSCs: MAP2 0 %;  $\beta$ III-tubulin 52 % (weak staining). **b** 1 week differentiated GSCs: MAP2 0.7 %;  $\beta$ III-tubulin 95 %. **c** 4 weeks differentiated GSCs: MAP2 2 %;  $\beta$ III-tubulin 89 %. **d** undifferentiated GSCs: nestin 97 %; GFAP 6 %. **e** 1 week differentiated GSCs: nestin 41 %; GFAP 29 %. **f** 4 weeks differentiated GSCs: nestin 28 %; GFAP 25 %. **g–i** Proliferation was reduced, shown by a lower proportion of Ki-67 positive cells after differentiation (Ki-67 positive nuclei shown as white due to merge with blue nuclear stain). *Blue*: Hoechst in all images. *Scale bar* 100  $\mu$ m. **j** Gene expression analyzed by qRT-PCR of undifferentiated, 1 week differentiated and 4 weeks differentiated GSC cultures.  $\beta$ III-tubulin was significantly up-regulated after 1 week differentiation, GFAP expression was highly increased after differentiation. Nestin expression was significantly reduced after 4 weeks differentiation. CD133 expression was significantly reduced with increasing differentiation. The *bars* represent experiments in triplicate or more. **k** Computerized counting of Ki-67 positive cells from a representative GSC culture.  $N = 4$  experiments and more than 600 cells in each differentiation state

to release of dye accumulated in the mitochondria (Fig. 3b). After the hypoxia period, FCCP was applied to determine which cells had remaining mitochondrial membrane potential. A further increase in fluorescence indicates that mitochondrial membrane potential was still to some degree preserved at this point. The proportion of cells showing remaining  $\Delta\Psi_m$  after hypoxia in undifferentiated GSCs was for T1 41.4 % (14.1–68.8), T2 57.6 % (41.9–73.4) and T3 73.6 % (44.6–102.6) (Fig. 3e–g).

One week differentiated GSCs also responded to 15 min hypoxia by some mitochondrial depolarization (Fig. 3c). However only a few of the cells were totally depolarized. One week differentiated cells with a preserved  $\Delta\Psi_m$  represented for T1 90.0 % (73.6–106.3), T2 88.3 % (68.2–108.5) and T3 93.3 % (74.8–111.8). Compared to the undifferentiated cells, the fraction of cells with complete loss of mitochondrial membrane potential were significantly lower among the 1 week differentiated GSCs of T1 and T2 ( $p < 0.05$ , ANOVA). The same trend was seen in T3, but not statistically significant.

In GSCs differentiated for 4 weeks (Fig. 3d) Rh123 fluorescence increased during hypoxia, demonstrating depolarization of the mitochondrial membrane. The majority of 4 week differentiated T1 and T2 GSCs did not preserve any mitochondrial membrane potential after 15 min hypoxia. In addition, the cells from T3 showed the same pattern of development compared to 1 week differentiated cells, however not statistically significant. The 4 weeks differentiated GSCs preserved mitochondrial

membrane potential after 15 min hypoxia in 41.4 % (2.8–80.0) of T1, 22.8 % (5.2–40.3) of T2 and 48.0 % (–9.2 to 105.2) of T3 (Fig. 3e–g). In two of the tumors the mitochondrial hypoxia tolerance was significantly lowered compared to 1 week differentiation (T1  $p < 0.05$ , T2  $p < 0.001$ , ANOVA). Representative time-lapse fluorescence images of undifferentiated, 1 week differentiated and 4 weeks differentiated GSCs are shown in Fig. 4 and Online resources 3, 4 and 5.

After finding increased tolerance to hypoxia in 1 week differentiated cells, we wanted to investigate whether differentiation changed the energy metabolism of the cells. As seen in Fig. 5a, undifferentiated GSCs had a low basal rate of oxygen consumption and acidification rate. OCR and ECAR were increased after both 1 and 4 weeks differentiation. However, the OCR/ECAR ratio was not significantly different between the groups. Further measurements were normalized to baseline values in order to enable comparison between the groups. Oligomycin was added to irreversibly block the mitochondrial ATP synthase/ATPase. Both production and consumption of ATP by the mitochondria were thus inhibited. The values recorded following this treatment are measures of the oxygen consumption needed to compensate for proton leakage across the inner mitochondrial membrane. The proton leak relative to basal metabolism was not significantly different between undifferentiated and differentiated cells.

FCCP treatment leads to uncoupling and thereby maximal oxygen consumption in the mitochondria. The difference between maximal and basal oxygen consumption is termed the reserve respiratory capacity (Fig. 5b). The relative reserve respiratory capacity was the highest in 4 week differentiated cells, and significantly less in 1 week differentiated and least in undifferentiated cells. The increased respiration capacity is due to enhanced complex I activity (Fig. 5d). Inhibition of mitochondrial ATP production by oligomycin combined with FCCP led to more increase in relative glycolysis (ECAR) in undifferentiated GSCs compared to 4 weeks differentiated cells (Fig. 5c).

In order to further characterize the mitochondrial function in undifferentiated and differentiated GSCs resting mitochondrial membrane potential was investigated. The mitochondrial membrane potential is high when activity is low and reduced if activity is high. In order to reduce bias due to differences in cell size, the ratiometric two color fluorescent probe JC-1 was chosen. Red and green fluorescence was measured by flow cytometry and the red/green ratio compared (Fig. 5e).  $\Delta\Psi_m$  was significantly different when comparing undifferentiated cells to both 1 week ( $p < 0.05$ ) and 4 weeks ( $p < 0.01$ ) differentiated cells. The difference between our one and 4 weeks differentiated cells was not statistically significant. JC-1 ratio of FCCP treated cells was used as a control of totally

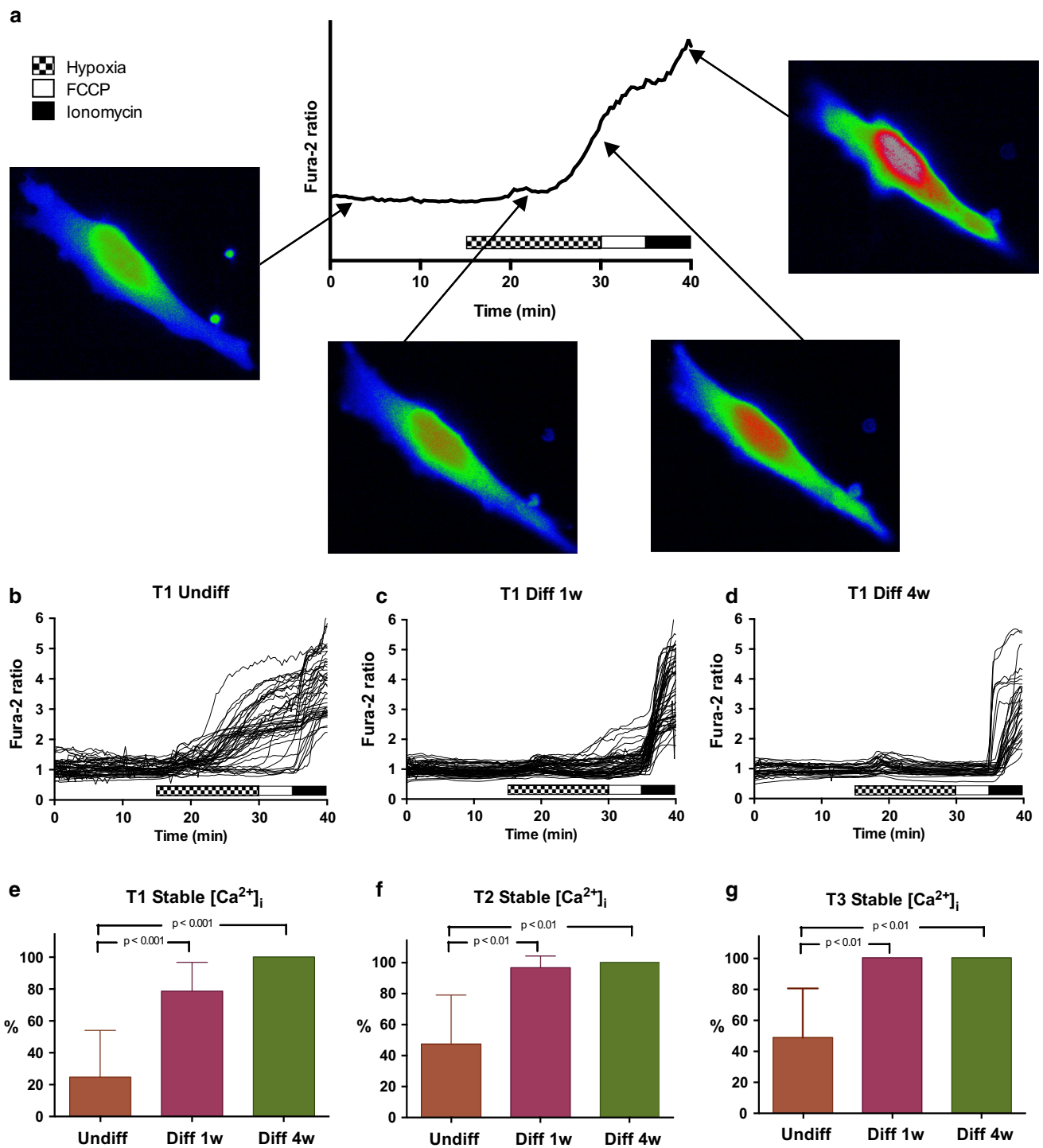


**Fig. 2**  $Ca^{2+}$  stability during hypoxia was improved after 1 week differentiation and sustained at 4 weeks. **a** Schematic presentation of a hypoxia experiment. Intracellular calcium change was recorded using Fura-2 staining and fluorescence time-lapse microscopy. Presented images are pseudocolor images of fura-2 ratio. Baseline recording show stable calcium levels. Calcium increase during hypoxia is shown by increased Fura-2 ratio. Application of Ionomycin at the end of experiments confirms the ability to detect calcium

changes. Fura-2 ratio measurements of **b** undifferentiated, **c** 1 week differentiated and **d** 4 week differentiated GSCs. For graphs of all three tumors, see Online Resource 1. **e–g** Proportions of cells that maintained stable intracellular calcium during 15 min hypoxia were significantly increased from undifferentiated to differentiated state in all three GSC cultures, which represent cells from three different patient samples. In all groups  $n \geq 5$  experiments and  $\geq 25$  cells

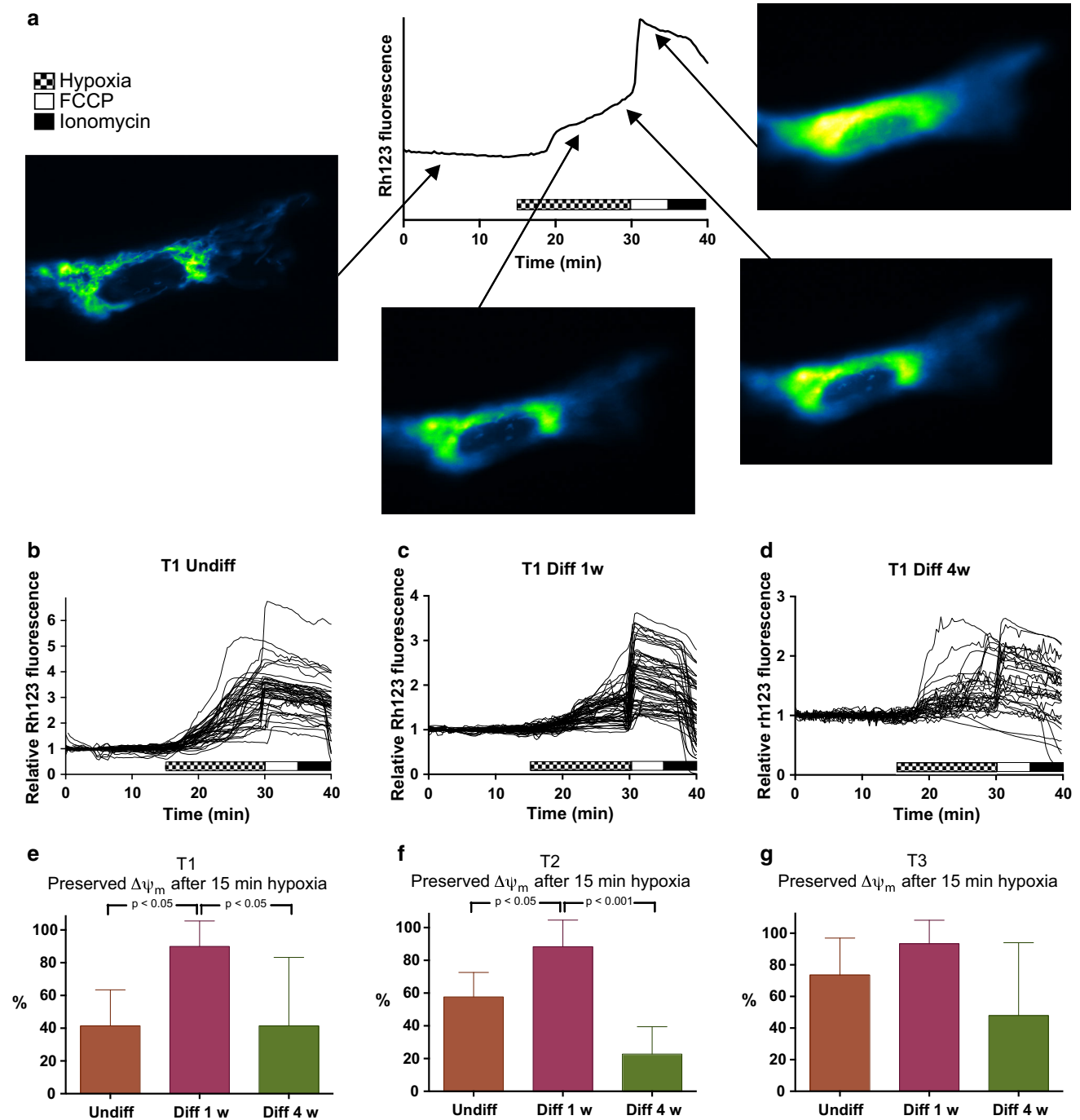


**Fig. 3** Mitochondrial hypoxia tolerance was improved only at 1 week differentiation. **a** Schematic presentation of a hypoxia experiment. Baseline recording shows stable  $\Delta\Psi_m$ . During hypoxia the fluorescence increases due to mitochondrial depolarization. After FCCP remaining  $\Delta\Psi_m$  is depolarized shown by further increase in fluorescence before decrease due to diffusion of rh123 out of the cell. **b, c, d** Traces of Rhodamine 123 fluorescence in the same cells as in Fig. 2 showing depolarization of mitochondrial membrane potential upon hypoxia and FCCP in **b** undifferentiated, **c** 1 week differentiated and **d** 4 week differentiated GSCs. The proportion of cells showing

preserved  $\Delta\Psi_m$  after hypoxia was in **b** undifferentiated GSCs 41.4 % (14.1–68.8), **c** 1 week differentiated GSCs 90.0 % (73.6–106.3) and **d** 4 weeks differentiated GSCs 41.4 % (2.8–80.0). For graphs of all three tumors, see Online Resource 2. **e–g** The bar graphs show for the different three tumors the proportion of cells that had preserved mitochondrial membrane potential after 15 min hypoxia, with significant increased hypoxia tolerance development from undifferentiated to 1 week differentiated state in and reversal of this to 4 weeks differentiation in tumor cultures T1 and T2. In all groups  $n \geq 5$  experiments and  $\geq 25$  cells



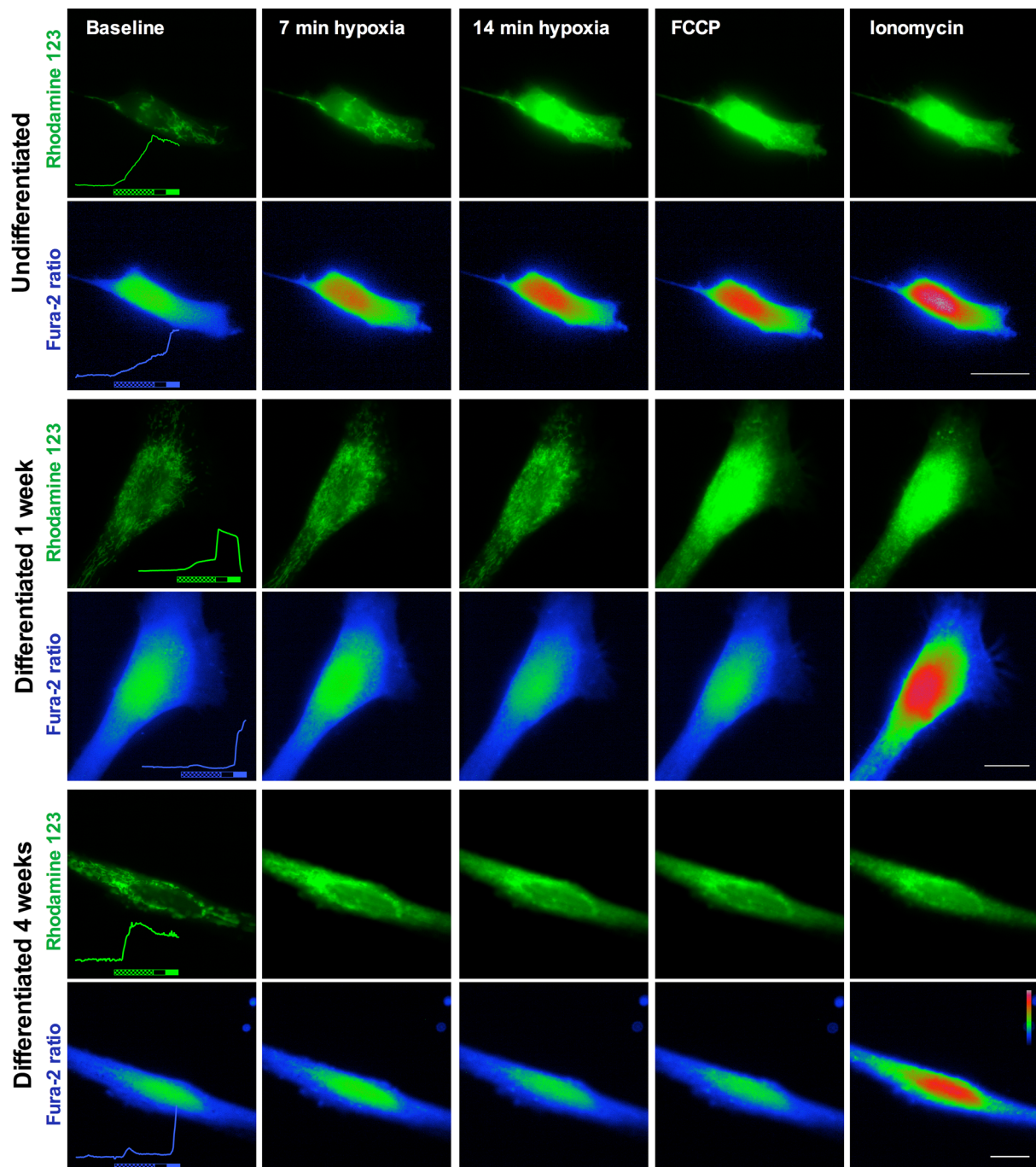


**Fig. 4** Representative time-lapse fluorescence microscopy images of undifferentiated, 1 week differentiated and 4 weeks differentiated GSCs exposed to 15 min hypoxia. Fura-2 is presented as pseudocolor ratio images. Traces of Rh123 fluorescence and Fura-2 ratio in the actual cells are presented as inset in the first images. Hypoxia, FCCP and Ionomycin are marked as in Figs. 2 and 3. Increasing fluorescence of Rh123 indicates mitochondrial membrane depolarization. Increasing fura-2 ratio indicates increase of intracellular calcium levels. The undifferentiated cell lost mitochondrial membrane potential and control of intracellular calcium during 15 min hypoxia. There was

no reaction to FCCP on mitochondrial membrane potential. The 1 week differentiated cell mitochondria are partially depolarized during hypoxia, but shows preserved potential by increase in Rh123 fluorescence at FCCP application. Intracellular calcium is stable through the hypoxic period. The 4 weeks differentiated cell has fully depolarized mitochondria after 15 min hypoxia, shown by no increase in Rh123 fluorescence after FCCP application. Intracellular calcium increased after release of extracellular calcium into the cell by ionomycin. Scale bars 20  $\mu$ m

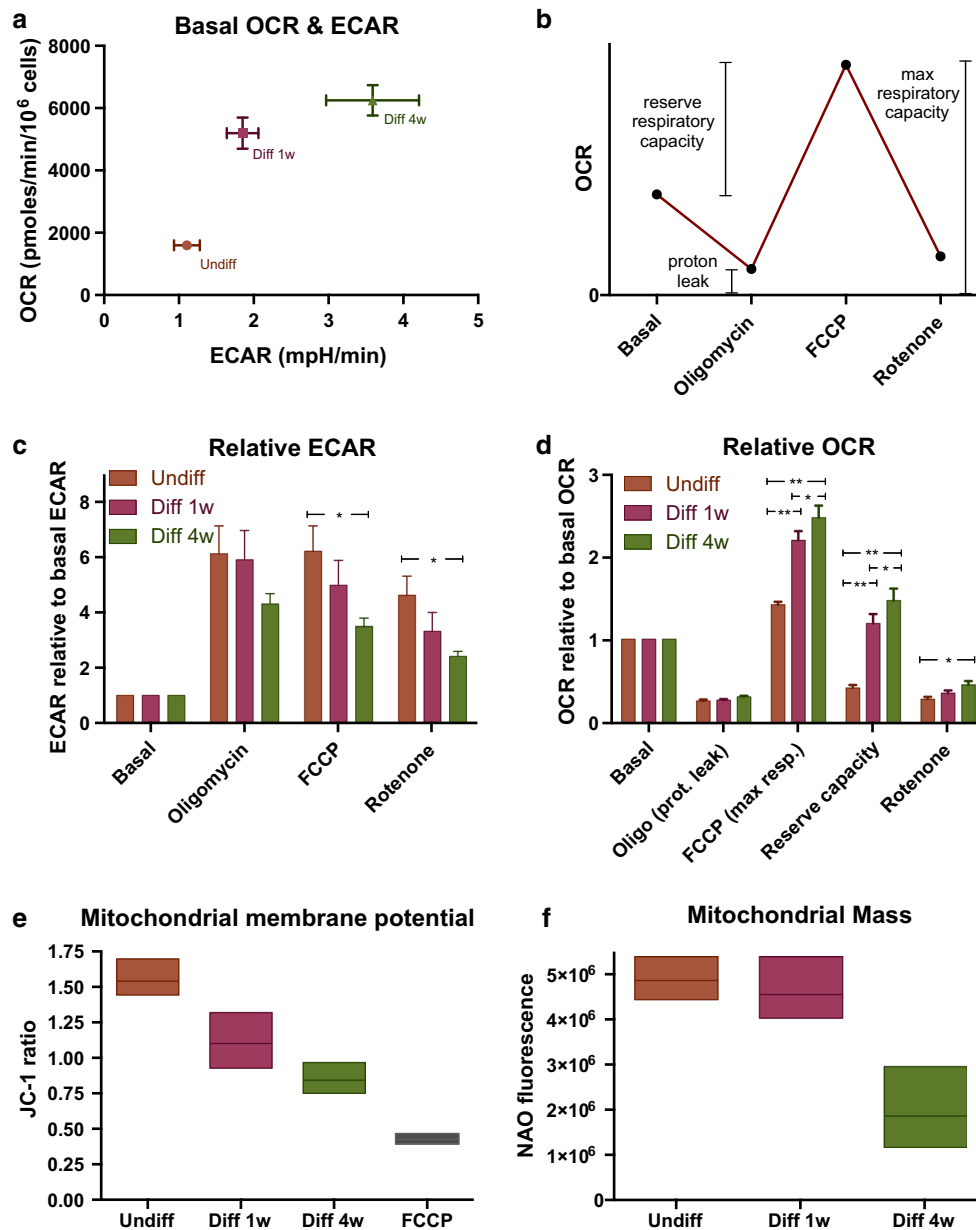


**Fig. 5** Respiration,  $\Delta\Psi_m$  and mitochondrial mass were changed by differentiation. Oxygen consumption rate (OCR) and extracellular acidification rate (ECAR) were measured simultaneously in cultures of undifferentiated, 1 and 4 weeks differentiated GSCs. The measurements were adjusted to actual cell count. **a** Basal metabolism show low absolute OCR and ECAR in undifferentiated cells, and increasing metabolic rate with increasing differentiation. **b** Schematic presentation of the events and measurements in the experiments: OCR after blocking of mitochondrial complex V by oligomycin shows the oxygen consumption used due to proton leak across the inner mitochondrial membrane. Reserve respiratory capacity is the

depolarized cells and was found significantly lower compared to all other groups.

The low oxygen consumption and lower maximal respiration in undifferentiated cells suggested a possible difference in mitochondrial contents in the cells. To compare

difference between max respiration induced by FCCP and basal level of oxygen consumption. **c, d** ECAR and OCR measurements normalized to baseline. **e**  $\Delta\Psi_m$  in undifferentiated and differentiated GSCs shown as JC-1 ratio measured by flow cytometry.  $\Delta\Psi_m$  was the highest in undifferentiated cells and decreased with increasing differentiation. FCCP treated cells as control. **f** Mitochondrial mass was assessed by Nonyl Acridine Orange and flow cytometry, and found similar in undifferentiated and 1 week differentiated cells, but decreased after 4 weeks differentiation. Arbitrary fluorescence units on the Y-axis. All experiments were performed at least three times

mitochondrial mass in undifferentiated and differentiated GSCs we stained fixed cells from each group with Nonyl Acridine Orange (NAO). NAO stains cardiolipin in the inner mitochondrial membrane in a linear relationship to mitochondrial membrane surface area and can thus be used

as an indicator of mitochondrial mass in the cell. Mitochondrial mass was found similar in undifferentiated and 1 week differentiated cells (no significant difference). Four week differentiated cells had significantly less NAO fluorescence compared to both undifferentiated and 1 week differentiated cells (both  $p < 0.01$ ), indicative of less mitochondrial mass in the long-term differentiated cells (Fig. 5f).

## Discussion

The main findings of this work were (a) undifferentiated GSCs did not tolerate acute hypoxia, (b) limited differentiation induced tolerance to acute hypoxia and (c) mitochondrial hypoxia tolerance was lost after prolonged differentiation. The lack of hypoxia tolerance in our most immature cells was not expected. Experiments on the neonatal brain have previously demonstrated hypoxia tolerance in immature brain cells [24, 38]. Based on this and previous reports of reduced mitochondrial activity in stem cells [39] and cancer cells [40–42], the most immature of our cells were expected to be the least oxygen dependent, and thus the most hypoxia tolerant. However, our results suggest that the most immature GSCs are oxygen dependent. This can be seen in coherence with the perivascular localization of GSCs in tumors [43]. The Warburg effect, i.e. impaired oxidative metabolism in cancer tissue [42], has been suggested evident in GSCs [44]. Our measurements of oxygen consumption (OCR) and lactate generation (ECAR; Fig. 5a) revealed a comparable relationship between oxidative and glycolytic metabolism in both undifferentiated and differentiated cells. Undifferentiated cells had the least relative reserve respiratory capacity (Fig. 5d), indicating a basal oxidative metabolism almost at maximum. Even though undifferentiated cells had the same mitochondrial mass as 1 week differentiated cells (Fig. 5f), the absolute basal oxygen consumption was significantly lower (Fig. 5a). Low absolute oxygen consumption in the most immature cells is in agreement with the findings of other groups [40, 45, 46], but also contrary to a recent study using a GBM cell line [47]. In controlled experiments there is an inverse proportional relationship between  $\Delta\Psi_m$  and respiration rate [48]. In our experiments, the highest  $\Delta\Psi_m$  was found in the undifferentiated cells (Fig. 5e). The high  $\Delta\Psi_m$  corresponds with the low basal oxygen consumption relative to mitochondrial mass found in the undifferentiated cells. This finding could fit with the Warburg theory of inhibited oxidative metabolism. However, the oxygen dependency and lack of increased glycolytic metabolism suggests a reason for doubt on the Warburg effect in these GSCs.

A majority of the GSCs subjected to 1 week of differentiation stimuli developed a tolerance to acute hypoxia.

These cells were able to preserve both calcium homeostasis and mitochondrial membrane potential during 15 min acute hypoxia. Maintenance of  $\Delta\Psi_m$  without oxygen is a process where the mitochondrial ATP synthase is reversed and consumes ATP to maintain a proton gradient across the inner mitochondrial membrane [49]. This is possible as long as ATP is available and the  $\Delta\Psi_m$  is not disrupted by other factors, such as the mitochondrial pore transition (MPT) [50], which can be induced by calcium overload. The 1 week differentiated cells did not show signs of calcium overload. The amounts of ATP needed to maintain  $\Delta\Psi_m$  without oxygen is dependent on the proton leak across the inner mitochondrial membrane. Such leakage is dependent upon the level of the  $\Delta\Psi_m$  and the expression of uncoupling proteins. Proton leak increase with increasing  $\Delta\Psi_m$ . The  $\Delta\Psi_m$  obtained by ATP synthase reversal is in the magnitude of approximately  $-80$  mV, while in normal respiration  $\Delta\Psi_m$  is about  $-150$  mV [51]. The proton leak at  $-80$  mV is relatively low. Our data on basal metabolism show similar relative proton leak in the undifferentiated and differentiated cells (Fig. 5d), indicating similar expression of uncoupling proteins. The finding of a superior mitochondrial hypoxia tolerance in the 1 week differentiated cells suggests that these cells have the best ability to maintain all ATP needs by non-oxidative metabolism. This is consistent with oligomycin sensitivity in GSC sphere culture, but not in adherent serum stimulated GSC derived cells [52]. Hypoxia tolerance is also found in glioblastoma cell line U-87 after induction to express the neural progenitor protein doublecortin (DCX) [53]. Transplantation of cells to the brain is a known hypoxic situation. In a previous study from our lab, predifferentiation of neural stem cells before transplantation to mice produced improved survival and integration of the graft [21]. Similarly a study on transplantation of embryonal and post-natal retinal cells found the best results using cells of limited maturation [22].

The 4 weeks differentiated cells did not show mitochondrial hypoxia tolerance. However, intracellular calcium was stable in all cells. This could indicate that in these cells, the mitochondria are fragile, but other cell functions can be maintained without oxidative ATP production. Basal  $\Delta\Psi_m$  was the lowest in this group. Some depolarization is seen in cells with very active mitochondrial metabolism [48]. It is also seen as a property of aging [54]. The absolute oxygen consumption was slightly higher in 4 weeks differentiated cells compared to 1 week, even though mitochondrial mass was less (Fig. 5f). This group also had the least relative increase in glucose utilization after inhibition of mitochondrial ATP-production by oligomycin (Fig. 5c). An already high dependence upon glycolytic metabolism could contribute to the increased hypoxia tolerance found in terms of stable intracellular calcium during hypoxia. Whether the

mitochondrial depolarization seen during hypoxia in this group induces any permanent damage is not clarified by this study, and needs further investigation. In hypoxia tolerant animals and neonatal mice, hypoxia induces a small and temporary increase of intracellular calcium [37], and this has been suggested as indicative of cell survival instead of late hypoxic death through apoptosis. Such calcium fluctuation has also been suggested as a signal in hypoxic preconditioning [55]. A small and temporary increase in intracellular calcium after 3–5 min hypoxia was seen in many of our differentiated GSCs (Fig. 2c, d, and Online Resource 1).

The in vitro culture conditions are always a possible confounder of results that are interpreted as relevant to true in vivo properties. However, our culture protocol does maintain stem cell properties, multipotency and tumorigenicity through multiple passages [25]. In contrast to traditional cancer cell lines, often cultured in as much as 10 % serum, our undifferentiated cells did not get serum supplements. Serum free culture conditions seem important for maintenance of tumor stem cell (TSC) properties [35]. Culture in ambient oxygen level is the common method, although ambient oxygen is actually hyperoxia to cells. Still, the cells preserve TSC properties [25]. To challenge cells with acute hypoxia we have used 0 % oxygen. Hypoxia experiments are often performed using 1–2 % oxygen levels. This is, however, closer to the physiologic oxygen tension, and especially in tumors low oxygen levels are common. Close to zero oxygen is needed for relevant acute hypoxia effects [56].

The clinical relevance of tumor hypoxia on CSCs is related to treatment resistance and malignant progression. Hypoxia dependent temozolomide resistance was recently shown in GSCs [46]. Differentiation has been suggested as a possible GBM treatment strategy [20]. Whether partially differentiated GSCs possess a malignant potential is uncertain. However, Ki-67 immunoreactivity in some of these cells (Fig. 1h) indicates a sustained proliferative ability [57]. A mechanism of bidirectional plasticity may exist. Induced reprogramming resulting in glioma propagating capacity has recently been shown in both mouse neurons [58] and differentiated GSCs [59].

Although having low basal oxygen consumption, our undifferentiated GSCs did not show hypoxia tolerance compared to partially differentiated cells of the same origin. Prolonged differentiation impaired mitochondrial hypoxia tolerance. The results of this study suggest that partly differentiated rather than undifferentiated GSCs possess the ability to utilize the therapy resistance offered by tissue hypoxia. This also implies that treatment of tumor hypoxia and hypoxia related resistance could be insufficient to eradicate GSCs. The knowledge on the malignancy potential of partially differentiated GSCs is still sparse.

This needs elucidation before development of in vivo differentiation therapy for glioblastoma.

**Acknowledgments** This study was funded by Oslo University Hospital, and has also received support from the Malthe foundation. We have had excellent working conditions, supplied by Ansgar O. Aasen and Sissel Reinlie. We are grateful for technical support by Emily Palmero, Ingunn Ramsnes, Sheryl Palmero and Zanina Grieg.

#### Compliance with Ethical Standards

**Conflict of interest** The authors declare that they have no conflict of interest.

**Open Access** This article is distributed under the terms of the Creative Commons Attribution 4.0 International License (<http://creativecommons.org/licenses/by/4.0/>), which permits unrestricted use, distribution, and reproduction in any medium, provided you give appropriate credit to the original author(s) and the source, provide a link to the Creative Commons license, and indicate if changes were made.

#### References

1. Helseth R, Helseth E, Johannesen TB, Langberg CW, Lote K, Ronning P, Scheie D, Vik A, Meling TR (2010) Overall survival, prognostic factors, and repeated surgery in a consecutive series of 516 patients with glioblastoma multiforme. *Acta Neurol Scand* 122(3):159–167. doi:10.1111/j.1600-0404.2010.01350.x
2. Singh SK, Clarke ID, Terasaki M, Bonn VE, Hawkins C, Squire J, Dirks PB (2003) Identification of a cancer stem cell in human brain tumors. *Cancer Res* 63(18):5821–5828
3. Galli R, Binda E, Orfanelli U, Cipelletti B, Gritti A, De Vitis S, Fiocco R, Foroni C, Dimeco F, Vescovi A (2004) Isolation and characterization of tumorigenic, stem-like neural precursors from human glioblastoma. *Cancer Res* 64(19):7011–7021. doi:10.1158/0008-5472.CAN-04-1364
4. Bao S, Wu Q, McLendon RE, Hao Y, Shi Q, Hjelmeland AB, Dewhirst MW, Bigner DD, Rich JN (2006) Glioma stem cells promote radioresistance by preferential activation of the DNA damage response. *Nature* 444(7120):756–760. doi:10.1038/nature05236
5. Murat A, Migliavacca E, Gorlia T, Lambiv WL, Shay T, Hamou MF, de Tribolet N, Regli L, Wick W, Kouwenhoven MC, Hainfellner JA, Heppner FL, Dietrich PY, Zimmer Y, Cairncross JG, Janzer RC, Domany E, Delorenzi M, Stupp R, Hegi ME (2008) Stem cell-related “self-renewal” signature and high epidermal growth factor receptor expression associated with resistance to concomitant chemoradiotherapy in glioblastoma. *J Clin Oncol* 26(18):3015–3024. doi:10.1200/JCO.2007.15.7164
6. Chen J, Li Y, Yu TS, McKay RM, Burns DK, Kernie SG, Parada LF (2012) A restricted cell population propagates glioblastoma growth after chemotherapy. *Nature* 488(7412):522–526. doi:10.1038/nature11287
7. Amberger-Murphy V (2009) Hypoxia helps glioma to fight therapy. *Curr Cancer Drug Targets* 9(3):381–390
8. Pistollato F, Abbadi S, Rampazzo E, Persano L, Della Puppa A, Frasson C, Sarto E, Scienza R, D’Avella D, Basso G (2010) Intratumoral hypoxic gradient drives stem cells distribution and MGMT expression in glioblastoma. *Stem Cells* 28(5):851–862. doi:10.1002/stem.415



9. Sathornsumetee S, Cao Y, Marcello JE, Herndon JE 2nd, McLendon RE, Desjardins A, Friedman HS, Dewhirst MW, Vredenburgh JJ, Rich JN (2008) Tumor angiogenic and hypoxic profiles predict radiographic response and survival in malignant astrocytoma patients treated with bevacizumab and irinotecan. *J Clin Oncol* 26(2):271–278. doi:[10.1200/JCO.2007.13.3652](https://doi.org/10.1200/JCO.2007.13.3652)
10. Spence AM, Muzi M, Swanson KR, O'Sullivan F, Rockhill JK, Rajendran JG, Adams TC, Link JM, Swanson PE, Yagle KJ, Rostomily RC, Silbergeld DL, Krohn KA (2008) Regional hypoxia in glioblastoma multiforme quantified with [18F]fluoromisonidazole positron emission tomography before radiotherapy: correlation with time to progression and survival. *Clin Cancer Res* 14(9):2623–2630. doi:[10.1158/1078-0432.CCR-07-4995](https://doi.org/10.1158/1078-0432.CCR-07-4995)
11. Brizel DM, Sibley GS, Prosnitz LR, Scher RL, Dewhirst MW (1997) Tumor hypoxia adversely affects the prognosis of carcinoma of the head and neck. *Int J Radiat Oncol Biol Phys* 38(2):285–289
12. Nordmark M, Alsner J, Keller J, Nielsen OS, Jensen OM, Horsman MR, Overgaard J (2001) Hypoxia in human soft tissue sarcomas: adverse impact on survival and no association with p53 mutations. *Br J Cancer* 84(8):1070–1075. doi:[10.1054/bjoc.2001.1728](https://doi.org/10.1054/bjoc.2001.1728)
13. Kolenda J, Jensen SS, Aaberg-Jessen C, Christensen K, Andersen C, Brunner N, Kristensen BW (2010) Effects of hypoxia on expression of a panel of stem cell and chemoresistance markers in glioblastoma-derived spheroids. *J Neurooncol*. doi:[10.1007/s11060-010-0357-8](https://doi.org/10.1007/s11060-010-0357-8)
14. Schulte A, Gunther HS, Phillips HS, Kemming D, Martens T, Kharbanda S, Soriano RH, Modrusan Z, Zapf S, Westphal M, Lamszus K (2011) A distinct subset of glioma cell lines with stem cell-like properties reflects the transcriptional phenotype of glioblastomas and overexpresses CXCR4 as therapeutic target. *Glia* 59(4):590–602. doi:[10.1002/glia.21127](https://doi.org/10.1002/glia.21127)
15. Louie E, Nik S, Chen JS, Schmidt M, Song B, Pacson C, Chen XF, Park S, Ju J, Chen EI (2010) Identification of a stem-like cell population by exposing metastatic breast cancer cell lines to repetitive cycles of hypoxia and reoxygenation. *Breast Cancer Res* 12(6):R94. doi:[10.1186/bcr2773](https://doi.org/10.1186/bcr2773)
16. Blazek ER, Foutch JL, Maki G (2007) Daoy medulloblastoma cells that express CD133 are radioresistant relative to CD133– cells, and the CD133+ sector is enlarged by hypoxia. *Int J Radiat Oncol Biol Phys* 67(1):1–5. doi:[10.1016/j.ijrobp.2006.09.037](https://doi.org/10.1016/j.ijrobp.2006.09.037)
17. Bayer C, Vaupel P (2012) Acute versus chronic hypoxia in gliomas: controversial data concerning time frames and biological consequences. *Strahlenther Onkol* 188(7):616–627. doi:[10.1007/s00066-012-0085-4](https://doi.org/10.1007/s00066-012-0085-4)
18. Rong Y, Durden DL, Van Meir EG, Brat DJ (2006) 'Pseudopalising' necrosis in glioblastoma: a familiar morphologic feature that links vascular pathology, hypoxia, and angiogenesis. *J Neuropathol Exp Neurol* 65(6):529–539
19. Kathagen A, Schulte A, Balcke G, Phillips HS, Martens T, Matschke J, Gunther HS, Soriano R, Modrusan Z, Sandmann T, Kuhl C, Tissier A, Holz M, Krawinkel LA, Glatzel M, Westphal M, Lamszus K (2013) Hypoxia and oxygenation induce a metabolic switch between pentose phosphate pathway and glycolysis in glioma stem-like cells. *Acta Neuropathol* 126(5):763–780. doi:[10.1007/s00401-013-1173-y](https://doi.org/10.1007/s00401-013-1173-y)
20. Piccirillo SG, Reynolds BA, Zanetti N, Lamorte G, Binda E, Broggi G, Brem H, Olivi A, Dimeco F, Vescovi AL (2006) Bone morphogenetic proteins inhibit the tumorigenic potential of human brain tumour-initiating cells. *Nature* 444(7120):761–765. doi:[10.1038/nature05349](https://doi.org/10.1038/nature05349)
21. Olstorn H, Varghese M, Murrell W, Moe MC, Langmoen IA (2011) Predifferentiated brain-derived adult human progenitor cells migrate toward ischemia after transplantation to the adult rat brain. *Neurosurgery* 68(1):213–222. doi:[10.1227/NEU.0b013e3181fd2c11](https://doi.org/10.1227/NEU.0b013e3181fd2c11) (discussion 222)
22. MacLaren RE, Pearson RA, MacNeil A, Douglas RH, Salt TE, Akimoto M, Swaroop A, Sowden JC, Ali RR (2006) Retinal repair by transplantation of photoreceptor precursors. *Nature* 444(7116):203–207. doi:[10.1038/nature05161](https://doi.org/10.1038/nature05161)
23. Wu P, Tarasenko YI, Gu Y, Huang LY, Coggeshall RE, Yu Y (2002) Region-specific generation of cholinergic neurons from fetal human neural stem cells grafted in adult rat. *Nat Neurosci* 5(12):1271–1278. doi:[10.1038/nn974](https://doi.org/10.1038/nn974)
24. Larsen GA, Skjellegrind HK, Vinje ML, Berg-Johnsen J (2008) Mitochondria are more resistant to hypoxic depolarization in the newborn than in the adult brain. *Neurochem Res* 33(9):1894–1900. doi:[10.1007/s11064-008-9664-2](https://doi.org/10.1007/s11064-008-9664-2)
25. Vik-Mo EO, Sandberg C, Olstorn H, Varghese M, Brandal P, Ramm-Petersen J, Murrell W, Langmoen IA (2010) Brain tumor stem cells maintain overall phenotype and tumorigenicity after in vitro culturing in serum-free conditions. *Neuro Oncol* 12(12):1220–1230. doi:[10.1093/neuonc/noq102](https://doi.org/10.1093/neuonc/noq102)
26. Varghese M, Olstorn H, Sandberg C, Vik-Mo EO, Noordhuis P, Nister M, Berg-Johnsen J, Moe MC, Langmoen IA (2008) A comparison between stem cells from the adult human brain and from brain tumors. *Neurosurgery* 63(6):1022–1033. doi:[10.1227/01.NEU.0000335792.85142.B0](https://doi.org/10.1227/01.NEU.0000335792.85142.B0) (discussion 1033–1024)
27. Larsen GA, Skjellegrind HK, Berg-Johnsen J, Moe MC (1077) Vinje ML (2006) Depolarization of mitochondria in isolated CA1 neurons during hypoxia, glucose deprivation and glutamate excitotoxicity. *Brain Res* 1:153–160. doi:[10.1016/j.brainres.2005.10.095](https://doi.org/10.1016/j.brainres.2005.10.095)
28. Duchen MR, Biscoe TJ (1992) Relative mitochondrial membrane potential and [Ca<sup>2+</sup>]<sub>i</sub> in type I cells isolated from the rabbit carotid body. *J Physiol* 450:33–61
29. Grynkiewicz G, Poenie M, Tsien RY (1985) A new generation of Ca<sup>2+</sup> indicators with greatly improved fluorescence properties. *J Biol Chem* 260(6):3440–3450
30. Benz R, McLaughlin S (1983) The molecular mechanism of action of the proton ionophore FCCP (carbonylcyanide p-trifluoromethoxyphenylhydrazone). *Biophys J* 41(3):381–398. doi:[10.1016/S0006-3495\(83\)84449-X](https://doi.org/10.1016/S0006-3495(83)84449-X)
31. Kamensky L, Jones TR, Fraser A, Bray MA, Logan DJ, Madden KL, Ljosa V, Rueden C, Eliceiri KW, Carpenter AE (2011) Improved structure, function and compatibility for Cell Profiler: modular high-throughput image analysis software. *Bioinformatics* 27(8):1179–1180. doi:[10.1093/bioinformatics/btr095](https://doi.org/10.1093/bioinformatics/btr095)
32. Cossarizza A, Baccarani-Contri M, Kalashnikova G, Franceschi C (1993) A new method for the cytofluorimetric analysis of mitochondrial membrane potential using the J-aggregate forming lipophilic cation 5,5',6,6'-tetrachloro-1,1',3,3'-tetraethylbenzimidazol carbocyanine iodide (JC-1). *Biochem Biophys Res Commun* 197(1):40–45
33. Maftah A, Petit JM, Ratinaud MH, Julien R (1989) 10-N nonyl-acridine orange: a fluorescent probe which stains mitochondria independently of their energetic state. *Biochem Biophys Res Commun* 164(1):185–190
34. Petit JM, Maftah A, Ratinaud MH, Julien R (1992) 10 N-nonyl acridine orange interacts with cardiolipin and allows the quantification of this phospholipid in isolated mitochondria. *Eur J Biochem* 209(1):267–273
35. Lee J, Kotliarova S, Kotliarov Y, Li A, Su Q, Donin NM, Pastorino S, Puro BW, Christopher N, Zhang W, Park JK, Fine HA (2006) Tumor stem cells derived from glioblastomas cultured in bFGF and EGF more closely mirror the phenotype and genotype of primary tumors than do serum-cultured cell lines. *Cancer Cell* 9(5):391–403. doi:[10.1016/j.ccr.2006.03.030](https://doi.org/10.1016/j.ccr.2006.03.030)
36. Budd SL, Nicholls DG (1996) Mitochondria, calcium regulation, and acute glutamate excitotoxicity in cultured cerebellar granule cells. *J Neurochem* 67(6):2282–2291

37. Bickler PE (2004) Clinical perspectives: neuroprotection lessons from hypoxia-tolerant organisms. *J Exp Biol* 207(Pt 18):3243–3249. doi:[10.1242/jeb.00977](https://doi.org/10.1242/jeb.00977)
38. Friedman JE, Haddad GG (1993) Major differences in Ca<sup>2+</sup> + i response to anoxia between neonatal and adult rat CA1 neurons: role of Ca<sup>2+</sup> + o and Na + o. *J Neurosci* 13(1):63–72
39. Chen CT, Hsu SH (1800) Wei YH (2010) Upregulation of mitochondrial function and antioxidant defense in the differentiation of stem cells. *Biochim Biophys Acta* 3:257–263. doi:[10.1016/j.bbagen.2009.09.001](https://doi.org/10.1016/j.bbagen.2009.09.001)
40. Zhou Y, Shingu T, Feng L, Chen Z, Ogasawara M, Keating MJ, Kondo S, Huang P (2011) Metabolic alterations in highly tumorigenic glioblastoma cells: preference for hypoxia and high dependency on glycolysis. *J Biol Chem* 286(37):32843–32853. doi:[10.1074/jbc.M111.260935](https://doi.org/10.1074/jbc.M111.260935)
41. Ye XQ, Li Q, Wang GH, Sun FF, Huang GJ, Bian XW, Yu SC, Qian GS (2011) Mitochondrial and energy metabolism-related properties as novel indicators of lung cancer stem cells. *Int J Cancer*. doi:[10.1002/ijc.25944](https://doi.org/10.1002/ijc.25944)
42. Warburg O (1956) On the origin of cancer cells. *Science* 123(3191):309–314
43. Calabrese C, Poppleton H, Kocak M, Hogg TL, Fuller C, Hamner B, Oh EY, Gaber MW, Finklestein D, Allen M, Frank A, Bayazitov IT, Zakharenko SS, Gajjar A, Davidoff A, Gilbertson RJ (2007) A perivascular niche for brain tumor stem cells. *Cancer Cell* 11(1):69–82. doi:[10.1016/j.ccr.2006.11.020](https://doi.org/10.1016/j.ccr.2006.11.020)
44. Michelakis ED, Sutendra G, Dromparis P, Webster L, Haromy A, Niven E, Maguire C, Gammer TL, Mackey JR, Fulton D, Abdulkarim B, McMurtry MS, Petruk KC (2010) Metabolic modulation of glioblastoma with dichloroacetate. *Sci Transl Med* 2(31):31–34. doi:[10.1126/scitranslmed.3000677](https://doi.org/10.1126/scitranslmed.3000677)
45. Vlashi E, Lagadec C, Vergnes L, Matsutani T, Masui K, Poulou M, Popescu R, Della Donna L, Evers P, Dekmezian C, Reue K, Christofk H, Mischel PS, Pajonk F (2011) Metabolic state of glioma stem cells and nontumorigenic cells. *Proc Natl Acad Sci USA* 108(38):16062–16067. doi:[10.1073/pnas.1106704108](https://doi.org/10.1073/pnas.1106704108)
46. Yuan S, Wang F, Chen G, Zhang H, Feng L, Wang L, Colman H, Keating MJ, Li X, Xu RH, Wang J, Huang P (2013) Effective elimination of cancer stem cells by a novel drug combination strategy. *Stem Cells* 31(1):23–34. doi:[10.1002/stem.1273](https://doi.org/10.1002/stem.1273)
47. Dickinson A, Yeung KY, Donoghue J, Baker MJ, Kelly RD, McKenzie M, Johns TG, St John JC (2013) The regulation of mitochondrial DNA copy number in glioblastoma cells. *Cell Death Differ* 20(12):1644–1653. doi:[10.1038/cdd.2013.115](https://doi.org/10.1038/cdd.2013.115)
48. Nicholls DG (1974) Hamster brown-adipose-tissue mitochondria. The control of respiration and the proton electrochemical potential gradient by possible physiological effectors of the proton conductance of the inner membrane. *Eur J Biochem* 49(3):573–583
49. Nicholls DG, Budd SL (2000) Mitochondria and neuronal survival. *Physiol Rev* 80(1):315–360
50. Zoratti M, Szabo I (1995) The mitochondrial permeability transition. *Biochim Biophys Acta* 1241(2):139–176
51. Chinopoulos C (2011) Mitochondrial consumption of cytosolic ATP: not so fast. *FEBS Lett* 585(9):1255–1259. doi:[10.1016/j.febslet.2011.04.004](https://doi.org/10.1016/j.febslet.2011.04.004)
52. Janiszewska M, Suva ML, Riggi N, Houtkooper RH, Auwerx J, Clement-Schatlo V, Radovanovic I, Rheinbay E, Provero P, Stamenkovic I (2012) Imp2 controls oxidative phosphorylation and is crucial for preserving glioblastoma cancer stem cells. *Genes Dev* 26(17):1926–1944. doi:[10.1101/gad.188292.112](https://doi.org/10.1101/gad.188292.112)
53. Santra M, Liu XS, Santra S, Zhang J, Zhang RL, Zhang ZG, Chopp M (2006) Ectopic expression of doublecortin protects adult rat progenitor cells and human glioma cells from severe oxygen and glucose deprivation. *Neuroscience* 142(3):739–752. doi:[10.1016/j.neuroscience.2006.06.065](https://doi.org/10.1016/j.neuroscience.2006.06.065)
54. Hagen TM, Yowe DL, Bartholomew JC, Wehr CM, Do KL, Park JY, Ames BN (1997) Mitochondrial decay in hepatocytes from old rats: membrane potential declines, heterogeneity and oxidants increase. *Proc Natl Acad Sci USA* 94(7):3064–3069
55. Bickler PE, Fahlman CS, Gray J, McKleroy W (2009) Inositol 1,4,5-triphosphate receptors and NAD(P)H mediate Ca<sup>2+</sup> + signaling required for hypoxic preconditioning of hippocampal neurons. *Neuroscience* 160(1):51–60. doi:[10.1016/j.neuroscience.2009.02.013](https://doi.org/10.1016/j.neuroscience.2009.02.013)
56. Papandreou I, Krishna C, Kaper F, Cai D, Giaccia AJ, Denko NC (2005) Anoxia is necessary for tumor cell toxicity caused by a low-oxygen environment. *Cancer Res* 65(8):3171–3178. doi:[10.1158/0008-5472.CAN-04-3395](https://doi.org/10.1158/0008-5472.CAN-04-3395)
57. Gerdes J, Schwab U, Lemke H, Stein H (1983) Production of a mouse monoclonal antibody reactive with a human nuclear antigen associated with cell proliferation. *Int J Cancer* 31(1):13–20
58. Friedmann-Morvinski D, Bushong EA, Ke E, Soda Y, Marumoto T, Singer O, Ellisman MH, Verma IM (2012) Dedifferentiation of neurons and astrocytes by oncogenes can induce gliomas in mice. *Science* 338(6110):1080–1084. doi:[10.1126/science.1226929](https://doi.org/10.1126/science.1226929)
59. Suva ML, Rheinbay E, Gillespie SM, Patel AP, Wakimoto H, Rabkin SD, Riggi N, Chi AS, Cahill DP, Nahed BV, Curry WT, Martuza RL, Rivera MN, Rossetti N, Kasif S, Beik S, Kadri S, Tirosh I, Wortman I, Shalek AK, Rozenblatt-Rosen O, Regev A, Louis DN, Bernstein BE (2014) Reconstructing and reprogramming the tumor-propagating potential of glioblastoma stem-like cells. *Cell* 157(3):580–594. doi:[10.1016/j.cell.2014.02.030](https://doi.org/10.1016/j.cell.2014.02.030)